SIRT6 overexpression potentiates apoptosis evasion in hepatocellular carcinoma via BCL2-associated X protein-dependent apoptotic pathway

Long-Kuan Ran[1, #],Yong Chen[3 #],Zhen-Zhen Zhang[4#],Na-Na Tao[1], Ji-Hua Ren[1], Li Zhou[5], Hua Tang[1], Xiang Chen[1], Ke Chen[1],Wan-Yu Li[1],Ai-Long Huang[1,2], Juan Chen[1]

[1]Key Laboratory of Molecular Biology for Infectious Diseases (Ministry of Education), Institute for Viral Hepatitis, Department of Infectious Diseases, The Second Affiliated Hospital, Chongqing Medical University, Chongqing, China; [2]Collaborative Innovation Center for Diagnosis and Treatment of Infectious Diseases, Zhejiang University, Zhejiang, China; [3]Department of Hepatobliliary Surgery, First Affiliated Hospital, Chongqing Medical University, Chongqing, China; [4]Department of Infectious Diseases, The Children's Hospital of Chongqing Medical University, Chongqing, China; [5]Department of Epidemiology, School of Public Health and Management, Chongqing Medical University, Chongqing , China

[#]These authors contributed equally to this work.

Running title: The role of SIRT6 in HCC

Key words: Hepatocelluar carcinoma; SIRT6; Apoptosis; BCL2-associated X protein

Corresponding Authors:

Prof. Juan Chen, The Second Affiliated Hospital and the Key Laboratory of Molecular Biology of Infectious Diseases designated by the Chinese Ministry of Education, Chongqing Medical University, Chongqing, China. Tel: (86)-02368818112, Email: yixin_xinyuan@163.com, FAX:(86)-02368486780.

Prof. Ai-Long Huang, The Second Affiliated Hospital and the Key Laboratory of Molecular Biology of Infectious Diseases designated by the Chinese Ministry of Education, Chongqing Medical University, Chongqing, China. Tel: (86)-02368818112, Email: ahuang1964@163.com, FAX:(86)-02368486780.

Conflict of Interest Disclosure: The authors disclose no potential conflicts of interest.

Statement of translational relevance

Optimal therapeutic strategies for hepatocellular carcinoma (HCC) patients are still challenging due to its high recurrence rate after surgical resection and chemotherapy resistance. Growing evidence shows that genetic and epigenetic alterations are involved in HCC progression, however, the underlying molecular mechanisms have not been fully elucidated. Here, we found SIRT6 was significantly upregulated in HCC tissues and upregulation of SIRT6 was significantly associated with increased tumor grade, tumor size, vascular invasion and shorter survival. Our *in vitro* and *in vivo* studies showed that gene silencing of SIRT6 suppressed cell proliferation and promoted cellular apoptosis by activating the Bax-dependent apoptotic signal pathway in HCC cells. Furthermore, SIRT6 knockdown could increase liver cancer cell sensitivity to chemotherapy drug doxorubicin. Collectively, the newly identified SIRT6-Bax axis partially illustrates the molecular mechanism of HCC progression and represents a novel potential therapeutic target for HCC treatment.

Abstract

Purpose: To characterize the functional role of SIRT6 in hepatocellular carcinoma (HCC).

Experimental Design: The expression of SIRT6 in 60 paired paraffin-embedded HCC tissues and adjacent nontumoral liver tissues was examined by immunohistochemistry. The expression of SIRT6 in 101 paired frozen HCC tissues and adjacent nontumoral liver tissues was analyzed by western blotting analysis and qPCR. The biological consequences of overexpression and knockdown of SIRT6 in HCC cell lines were studied *in vitro* and *in vivo*.

Results: SIRT6 expression was frequently upregulated in clinical HCC samples and that its expression was highly associated with tumor grade *(p*=0.02), tumor size (*p*=0.02), vascular invasion *(p*=0.004) and shorter survival (*p*=0.024). Depletion of SIRT6 from multiple liver cancer cell lines inhibited their growth and induced apoptosis *in vitro*. At the molecular level, we observed that the activation of the BCL2-associated X protein (Bax) signaling pathway, a major pathway that determines cancer cell apoptosis, is regulated by SIRT6 via its deacetylase activity. SIRT6 was recruited to the promoter of Bax, where it deacetylated histone 3 lysine 9 (H3K9) and suppressed its promoter activity. Binding of transcription factors (p53 and E2F-1) to Bax promoter was also generally increased in SIRT6-depleted cells. In mouse xenografts, SIRT6 suppression inhibited tumor growth and induced apoptosis. Finally, there is a negative correlation between SIRT6 and Bax mRNA expression in human HCC samples.

Conclusions: SIRT6 is an important pro-tumorigenic factor in liver carcinogenesis. Thus, the therapeutic targeting of SIRT6 may offer options for HCC treatment.

Introduction

Hepatocellular carcinoma is the third most frequent cause of cancer-related deaths worldwide, and its incidence rate is increasing (1). Despite progress in the diagnosis and treatment of HCC, its biology remains poorly understood, limiting patient outcome overall. Although this disease is biologically heterogeneous, the dysregulation of cellular proliferation and of apoptosis occurs frequently and contributes to the malignant phenotype (2). Defects in and the disruption of the death regulator pathway in cancer cells contribute to resistance to anticancer therapies (3). Therefore, greater understanding of how cancer cell evade death stimuli is urgently needed for the development of new therapeutic targets for HCC treatment.

The sirtuin (SIRT) family of NAD^+-dependent protein deacetylases has been implicated in life-span regulation in yeast, worms, and flies (4). Seven members of the SIRT family (SIRT1-SIRT7) have been identified in mammals. SIRT6 is a nuclear NAD^+-dependent deacetylase that regulates multiple molecular pathways to modulate DNA repair, telomere integrity and aging. SIRT6 regulates double-strand break (DSB) repair by recruiting SNF2H to DNA break sites (5), deacetylating the DSB-resection protein CtIP (6) and activating poly(ADP-ribose) polymerase 1(PARP1) under oxidative stress(7). SIRT6 specifically deacetylates histone H3 lysine 9 (H3K9) on telomeric chromatin, which is required for telomere maintenance (8). SIRT6 also attenuates NF-kB signaling *via* H3K9 deacetylation, which is an important regulator of aging-related cellular processes (9). Emerging evidence has also implicated SIRT6 in the development of various cancers, including breast cancer (10), skin cancer (11), prostate cancer (12), lung cancer (13), pancreatic cancer (14) and gliomas (15). SIRT6 regulates tumorigenesis by directly interacting with oncogenic proteins or by modulating the acetylation of H3K9 in oncogene promoters (15-18). However, the role of SIRT6 in HCC remains unclear.

We previously reported that SIRT1 and SIRT2 are critical participants in HCC development. SIRT1 is essential for proliferation and telomere maintenance (19), whereas SIRT2 mediates the epithelial-mesenchymal transition (EMT) of cancer cells

(20). In the present study, we found that SIRT6 was upregulated in a subset of HCC tissues and cell lines. SIRT6 overexpression in primary HCC tumors correlated with tumor size and grade. Furthermore, we discovered an oncogenic function of SIRT6 in HCC that involved the inhibition of cell apoptosis *via* the Bax-dependent signaling pathway *in vitro* and *in vivo*.

Materials and methods

Plasmids and antibodies

SIRT6 short hairpin RNA (shSIRT6-1 and shSIRT6-2) or nontargeting shRNA (shCont) were purchased from Shanghai Genechem Company Limited. Sequences of shSIRT6-1 and shSIRT6-2 are 5'-GCTACGTTGACGAGGTCATGA-3' and 5'-GCCTCTGACTTGCTGTGTTGT-3'. Sequence of shCont is 5'-GCAACAAGATG AAGAGCACCAA-3'. Anti-SIRT6 (NB100-2522) and Anti-Bax (NBP1-88682) were obtained from Novus Biologicals (Littleton, CO). Anti-Bax (#5023S), anti-COX IV (#4850), anti-Smac (#2954S), anti-Histone H3 (#3638), anti-Histone H4 (#07-327), anti-Bcl-2 (#2870), anti-Cytochrome C (#4280S), anti-PARP (#9542), anti-cleaved PARP (#5625) and anti-Caspase 9 (#9502), anti-E2F-1 (#3742), anti-p53 (#2527), anti-Acetyl-Lyine (#9441), anti-Caspase 3 (#9665) and anti-Cleaved caspase-3(#9664) were obtained from Cell Signaling Technology (Danvers, MA). Anti-acetyl-Histone H3 (Ac-Lys^{9}) (07-352) and anti-acetyl-Histone H4 (Ac-Lys^{16}) (07-329) were from Millipore (Billerica, MA). Anti-β-Actin (sc-1616) and anti-GAPDH (sc-365062) were purchased from Santa Cruz Biotechnology (Santa Cruz, CA). The plenti-c-Myc-DDK-SIRT6 expression vector was obtained from OriGene (Rockville, MD). Small interfering RNAs (siRNAs) targeting Bax and siRNAs with scrambled sequences were obtained from Invitrogen (Carlsbad, CA).

Cell culture

HepG2, PLC/PRF/5, SK-Hep-1 and Hep3B cells were obtained from American Type Culture Collection. Huh-7 cell line was acquired from the Health Science Research Resource Bank (Osaka, Japan). MIHA cell line was obtained from Prof. Ben C.B. Ko (The Hong Kong Polytechnic University), SMMC-7721 cell line was obtained from Prof. Ni Tang (Chong Qing medical University). HepG2, PLC/PRF/5, SK-Hep-1, Huh-7, SMMC-7721, Hep3B, and MIHA cell lines were cultivated in Dulbecco's modified Eagle's medium (DMEM) containing 10% fetal bovine serum (Gibco BRL, Grand Island, NY). HepG2 was maintained in MEM with 10% FBS. Primary human hepatocytes (PHHs) were purchased from Sciencell Research

laboratories and cultured in hepatocyte medium (Sciencell, Carlsbad, CA,). All cells were cultivated at 37°C in 5% CO_2. Cells were authenticated by short tandem repeat (STR) fingerprinting by Beijing Microread Genetics Company Limited recently.

HCC specimens

A set of 101 pairs of primary and corresponding adjacent nontumoral liver tissues were collected from the First Affiliated Hospital of Chongqing Medical University. The study protocol conformed to the ethical guidelines of the 1975 Declaration of Helsinki and was approved by the Clinical Research Ethics Committee of Chongqing Medical University. Total RNA and proteins were obtained from these specimens.

Co-immunoprecipitation assay and western blot analysis

Cells were harvested and lysed with RIPA lysis buffer containing a protease inhibitor cocktail (Roche Diagnostics, Indianapolis, IN). Then, the lysates were precipitated using protein magnetic beads (Millipore). For western blotting analysis, the lysates were separated by SDS-PAGE and transferred onto a nitrocellulose membrane. The membrane was then blocked with 5% non-fat milk for 1 h and incubated with relevant primary antibodies overnight at 4°C. The blots were developed using ECL western blotting reagents (Millipore). Band intensities of western blot were quantified by ImageJ v1.37 software.

Real-time quantitative PCR (qPCR)

Total RNA was extracted using TRIzol® Reagent (Invitrogen). cDNA was synthesized from 1μg of total RNA using an iScript™ cDNA Synthesis Kit (Bio-Rad, Richmond, Calif.). Relative gene expression levels following different treatments were determined using FastStart Universal SYBR Green Master Mix (Roche Diagnostics) with β-actin mRNA as an endogenous control. Values represent the means ± the standard deviations (SD) of three independent experiments. The expression values of target genes were calculated by using the $2^{-\Delta\Delta Ct}$ method. The primers were designed by our group and are listed in Table S1.

Chromatin immunoprecipitation (ChIP) assay

ChIP assays were performed with genomic DNA samples from cross-linked cells using a specific antibody according to the manufacturer's protocol (Millipore). A region of the Bax promoter was amplified from the immunoprecipitated DNA samples by PCR using the sense primer F 5'-TAAAAATTAACCAGGGGCGG-3' and the antisense primer R 5'-TCACTGTGTTGCCCAGGCTG-3'.

Cell proliferation assay

Cell proliferation in response to SIRT6 silencing or overexpression was determined by a trypan blue exclusion assay (Thermo Fisher Scientific, Waltham, MA). DNA synthesis was examined using a Click-iT® EdU Imaging Kit (Invitrogen) according to the manufacturer's instructions.

Colony formation assay and soft agar assay

The colony formation assay and soft agar assay have been described previously (19).

Flow cytometry

Cell apoptosis was analyzed by fluorescence-activated cell sorting (FACS) analysis as described previously (21).

Extraction of mitochondria and nuclear proteins

Nuclear proteins were purified using NE-PER® Nuclear and Cytoplasmic Extraction Reagents (Thermo Fisher Scientific) according to the manufacturer's instructions. Mitochondrial proteins were extracted using the Mitochondria/Cytosol Fraction Kit (Abcam, Cambridge, MA) according to the manufacturer's instructions.

Immunofluorescence and immunohistochemistry

SK-Hep-1 cells infected with lentivirus expressing shCont or shSIRT6 were seeded on coverslips, fixed in 4% paraformaldehyde and permeabilized using 0.5% Triton X-100. Then, the cells were incubated with rabbit anti-Bax antibody (Novus Biologicals; Dilution 1:100) and a fluorescein isothiocyanate (FITC)-coupled anti-rabbit secondary antibody. The cells were counterstained with DAPI to label the nuclei and examined by fluorescence microscopy (Leica TCS SP2).

Immunohistochemistry (IHC) was performed on paraffin-embedded sections. The tissue sections were deparaffinized, rehydrated, and microwaved-heated in sodium citrate buffer (10 mM, pH 6.0) for antigen retrieval. Then, the slides were

incubated with primary antibody (anti-Bax, 1:50; anti-Ki67, 1:100; anti-SIRT6, 1:200; anti-cleaved PARP, 1:200). DAB staining was used for detecting immunoreactivity (Dako, Carpinteria, CA). Counterstaining was performed using hematoxylin. The scoring of SIRT6 in HCC tissues was carried out by two independent pathologists according to the proportion of tumor cells with positive nuclear staining: 0 (<10%); 1 (10–30%); 2 (30–50%); 3 (>50%). HScore takes into consideration the intensity of the staining and the percentage of positive cells per the formula: HScore = 1×(% light staining) + 2×(% moderate staining) + 3×(%strong staining). HScores range from 0 to 300 (22).

Luciferase reporter assay

Distinct lengths of the Bax promoter fragment were subcloned into the pGL3-basic vector to produce pGL3-982, pGL3-803, pGL3-588, pGL3-389 and pGL3-213. These different vectors were co-transfected with shCont or shSIRT6. pRL-TK was co-transfected to normalize the transfection efficiency. Luciferase activity was measured using the Dual-Luciferase Reporter Assay System (Promega, Madison, WI) according to the manufacturer's instructions.

Animal model

Male BALB/c nude mice (4 weeks of age) received single subcutaneous flank injection of SK-Hep-1 cells suspended in 200μL DMEM/Matrigel (1:1 mixture). Tumor growth was monitored by bidimensional measurements using a caliper. Tumor–bearing mice were sacrificed 4 weeks after inoculation, and the tumors were removed for further study.

Statistical analysis

The SIRT6 expression levels in HCC and nontumoral liver tissues were compared using Student's paired *t*-test. Correlations between SIRT6 and individual clinicopathologic parameters were evaluated using a nonparametric chi-square test and Spearman's σ rank test. Kaplan-Meier's method was used to estimate the survival rates for SIRT6 expression. Equivalences of the survival curves were tested by log-rank statistics. All statistical analyses were performed using SPSS 19.0 software (IBM Corporation, USA).

Results

SIRT6 expression in human HCC

First, we analyzed SIRT6 expression patterns in 8 cell lines, including 6 HCC cell lines (Huh-7, HepG2, PLC/PRF/5, SMMC-7721, Hep3B and SK-Hep-1), one immortalized liver cell line (MIHA) and primary human hepatocyte (PHH). SIRT6 was almost undetectable in PHH, whereas high-level expression of SIRT6 was observed in the 6 HCC cell lines at both the mRNA and protein levels (Fig.1A-B).

Next, we determined SIRT6 expression in 60 paired paraffin-embedded HCC tissues and adjacent nontumoral livers by using immunohistochemistry. SIRT6 immunoreactivity was graded as negative (score 0), low (score 1–2) and high (score 3). In the 60 cases examined, positive SIRT6 expression was detected in 25/60 (41.6%) HCC tissues (Fig.1C). In contrast, SIRT6 staining was only detected in 9/60 (15%) adjacent nontumoral liver. Among the 25 positive HCC samples, 15 showed low staining and 10 showed strong staining of SIRT6. SIRT6 expression was further analyzed in 101 pairs of frozen HCC and adjacent nontumoral liver tissues by using western blotting analysis. SIRT6 overexpression was detected in 67/101 (66%) of HCCs compared to their adjacent nontumoral liver tissues (Fig. 1D and Supplementary Fig. 1). Furthermore, the average SIRT6 protein levels were significantly higher in tumor tissues relative to nontumoral liver tissues, indicating that SIRT6 was frequently overexpressed in HCC (Fig. 1E). We also compared SIRT6 mRNA levels in these samples by qPCR. SIRT6 mRNA levels were significantly upregulated in HCC tissues compared with nontumoral liver tissues (Fig. 1F), suggesting that SIRT6 overexpression in HCC is regulated in a transcription-dependent manner. Correlative analysis of SIRT6 protein levels with clinicopathologic features suggested significant association between increased SIRT6 expression and tumor size (p=0.02), tumor grade (p=0.02) and vascular invasion (p=0.004) (Table 1). Among these 101 HCCs, detailed survival information was available for 53 cases. Kaplan-Meier analysis revealed that patients with high SIRT6 expression levels in tissues had significantly shorter overall survival rates than those

with low SIRT6 expression (p=0.024) (Fig. 1G).

SIRT6 depletion in HCC cells inhibited proliferation and induced apoptosis

We analyzed the cellular loss-of-function phenotype *via* lentivirus-mediated shRNA interference to address the functional importance of SIRT6 in HCC development. Two independent shRNAs (shSIRT6-1 and shSIRT6-2) induced efficient SIRT6 knockdown in four HCC cell lines (PLC/PRF/5, SMMC-7721, Huh-7 and SK-Hep-1) compared with scrambled shRNA (shCont)-infected cells (Fig. 2A). The loss of SIRT6 significantly decreased the proliferation rate of all HCC cell lines examined (Fig. 2B). Furthermore, SIRT6 knockdown reduced the numbers and sizes of SK-Hep-1 cell colonies as determined by a colony formation assay (Fig. 2C). EdU staining also indicated that the loss of SIRT6 dramatically inhibited DNA synthesis (Fig. 2D).

Next, we determined if SIRT6 plays a role in the regulation of cell death. AnnexinV/PI assays indicated a dramatic increase in the apoptosis rate in SIRT6-depleted cells compared to their respective controls (Fig. 2E). SIRT6 depletion-induced apoptosis was further evidenced by enhanced poly(ADP-ribose) polymerase (PARP) cleavage and Caspase-3 cleavage (Fig. 2F). Additionally, we further examined the potential role of SIRT6 in resistance to the DNA-damaging agent doxorubicin. SIRT6 silencing promoted doxorubicin-induced apoptosis in Huh-7 and SK-Hep-1 cells, as evidenced by the AnnexinV/PI assays and by PARP cleavage (Supplementary Fig. 2A-B). Together, these data suggest that SIRT6 may play a role in the regulation of HCC proliferation and apoptosis.

SIRT6 overexpression in immortalized liver cell line promoted cell proliferation

To further elucidate the oncogenic role of SIRT6 in HCC tumorigenesis, we infected immortalized liver cell line (MIHA) with lentivirus expressing SIRT6, $SIRT6^{H133Y}$ (deacetylase inactive form of SIRT6) or vector. MIHA cells overexpressing wildtype SIRT6 exhibited increased growth rates (Supplementary Fig.3A) and enhanced DNA synthesis (Supplementary Fig. 3B) compared with control cells. Moreover, wild type SIRT6 overexpression in MIHA cells promoted the

anchorage-dependent growth of these cells as determined by a soft agar assay (Supplementary Fig. 3C). Although SIRT6 overexpression alone had no effect on MIHA cell apoptosis, this overexpression significantly enhanced MIHA cell resistance to apoptosis in response to doxorubicin treatment (Supplementary Fig. 3D). However, the expression of deacetylase inactive form of SIRT6 ($SIRT6^{H133Y}$) had no effect on cell growth and cell apoptosis. These data suggested the oncogenic function of SIRT6 dependent on its deacetylase activity.

SIRT6 regulated Bax signaling in HCC cells

To elucidate the underlying mechanisms by which SIRT6 regulates apoptosis in HCCs, we first examined alterations in apoptosis signal transduction in cells with or without SIRT6 depletion by mRNA microarray. Intriguingly, gene expression profiling indicated that SIRT6 silencing resulted in significant alterations in the Bax-mediated proapoptotic pathway (Supplementary Fig. 4).We performed real-time PCR coupled with western blot analysis to validate the screening results. We observed strong enhancement of Bax mRNA and protein levels, a key effector that initiates mitochondria-mediated cell death, in SIRT6-depleted cells (Fig. 3A). In contrast, SIRT6 overexpression in MIHA cells inhibited Bax expression (Fig. 3A). The activation of Bax in SIRT6-depleted cells was associated with a considerable decrease in the anti-apoptotic molecule Bcl-2 and with the accumulation of cytochrome c and second mitochondria-derived activator of caspases (Smac), accompanied by a more active form of Caspase-9, which are components of Bax signaling (Fig. 3B). Bax undergoes a conformational change that leads to its translocation to the mitochondrial membrane in response to apoptotic stimuli. Therefore, we examined the subcellular localization of Bax *via* immunofluorescence staining and biochemical subcellular fractionation. Immunofluorescence analysis revealed that Bax exhibited a diffuse staining pattern in control cells; this pattern indicated both cytosolic and nuclear localization. In contrast, Bax translocated to the cytosol and accumulated in mitochondria of SIRT6-depleted cells (Fig. 3C). Consistent with the immunofluorescence data, SIRT6 knockdown resulted in the marked redistribution of

Bax to mitochondria (Fig. 3D). These findings suggest that the anti-apoptotic activity of SIRT6 may be associated with the inhibition of Bax expression and with the blockage of its mitochondrial translocation.

To test this possibility, we knockdown Bax expression in SK-Hep-1 cells that were stably expressing shSIRT6. Impaired cell growth induced by SIRT6 silencing was substantially restored by the depletion of Bax proteins (Fig. 3E). Importantly, both AnnexinV/PI and PARP cleavage analyses indicated that Bax silencing significantly reduced apoptosis that was initiated by SIRT6 knockdown (Fig. 3F-G).Together, these data support the notion that SIRT6 regulates HCC cell growth and apoptosis by regulating Bax signaling.

SIRT6 deacetylated histone H3 lysine 9 in the Bax promoter

We hypothesized that SIRT6 may regulate Bax gene transcription in HCC cells by interacting with its promoter. To test this hypothesis, we first identified the Bax promoter core region. Various lengths of the Bax 5'-flanking region, including-590/+391(pGL3-982), -411/+391(pGL3-803), -196/+391(pGL3-588), +3/+391(pGL3-389), and +179/+391(pGL3-213), were cloned and transiently transfected into SK-Hep-1, Huh-7 and MIHA cells. A dual luciferase reporter assay indicated that all five Bax promoter-driven luciferase constructs exhibited higher luciferase activities in MIHA cell, in which SIRT6 expression is low (Fig. 4A). Construct pGL3-982 exhibited maximum luciferase activity, while pGL3-389 exhibited a robust reduction in luciferase activity, indicating that the -196/+3 region is the core region of the Bax promoter (Fig. 4A). Cotransfection of shRNA targeting SIRT6 with various constructs or with pGL3-basic was performed to determine the changes in luciferase activity. The data demonstrated that the regulatory site of SIRT6 is located at -196/+3 of Bax promoter, which is consistent with the core region of the *Bax* promoter (Fig. 4B).

In the context of gene expression, acetylated H3K9 is indicative of an actively transcribed gene, whereas H3K9 deacetylation is associated with gene repression. Previously, SIRT6 was reported to be a histone H3 lysine 9(H3K9) deacetylase (8, 9). Therefore, we determined whether SIRT6 is required for the deacetylation of H3K9 in

the Bax promoter. The ChIP assay revealed that SIRT6 was recruited to the Bax promoter region in HCC cells (Fig. 4C). H3K9 acetylation in the promoter of Bax was induced in SIRT6-depleted cells, which was consistent with transcriptional induction. In contrast, SIRT6 overexpression resulted in the hypoacetylation of the Bax promoter (Fig. 4D). However, no change in the acetylation status was observed at the histone H4 lysine16 in response to SIRT6 depletion or overexpression (Fig. 4D). Then, we asked whether H3K9 hyperacetylation of the Bax promoter in SIRT6-depleted cells affected its accessibility to DNA binding factor. The transcription factors p53 and E2F1 were selected based on published data. The ChIP assay revealed that the occupancy of p53 and E2F-1 in the Bax promoter was significantly enhanced in SIRT6-depleted cells. Together, these data suggest that SIRT6 is recruited to the Bax promoter to deacetylate H3K9, affecting its accessibility to transcription factors (Fig. 4E).

SIRT6 knockdown inhibits tumor growth and induced apoptosis *in vivo*

To investigate whether SIRT6 knockdown in HCC cells suppresses tumorigenicity *in vivo*, SK-Hep-1 cells infected with lentivirus expressing vector, shSIRT6 and shSIRT6+shBax were xenografted into nude mice subcutaneously. The growth rate of tumors derived from shSIRT6-infected cells was reduced significantly compared to vector-infected cells (Fig. 5A). Similarly, SIRT6 knockdown significantly inhibited both the size and weight of tumors whereas the effect was attenuated by the Bax suppression (Fig. 5B-C). SIRT6 knockdown in tumors tissues was associated with increased levels of cleaved PARP and decreased level of the cell proliferation marker Ki-67, and the effect was partially reversed by Bax knockdown (Fig. 5D). These data suggested that the SIRT6 knockdown in tumor cells can suppress tumor growth and induce apoptosis *in vivo*. Finally，we also examined SIRT6 and Bax mRNA in 101 HCC tissues that has been used to determine the relevance of SIRT6-regulated Bax pathway in human subjects. Correlative analysis further revealed a negative correlation between SIRT6 mRNA and Bax mRNA levels (Spearman's rank=-0.39, $P<0.001$). These data suggested that the SIRT6-Bax regulator axis might exist *in vivo* (Fig.5E).

Discussion

The role of SIRT6 in tumor development is controversial. A loss of SIRT6 in mouse embryonic fibroblasts (MEFs) led to tumor formation independent of oncogene activation, suggesting that SIRT6 may be a tumor suppressor (18). Furthermore, SIRT6 downregulation was observed in human pancreatic ductal adenocarcinomas (18), colorectal carcinomas and head and neck cancers (23). However, SIRT6 has been implicated as an oncogene in skin cancer (11)and prostate cancer (12). SIRT6 is upregulated in human skin cancer, where it promotes skin tumorigenesis by regulating COX-2 expression (11). SIRT6 is overexpressed in prostate cancer, and the inhibition of SIRT6 in prostate cancer reduces cell viability and increases sensitivity to chemotherapeutics (12). Taken together, these findings suggest that SIRT6 is both tumor suppressive and an oncogenic depending on the context and gene dose.

Regarding the role of SIRT6 in HCC, discrepancies still exist between the findings of our study and of other groups. Marquardt et al. noted a significant reduction of SIRT6 in HCC specimens based on analysis of a publically available cancer microarray database (24). These researchers further observed a reduction in SIRT6 mRNA expression in 45% (24/53) of HCC specimens from their recently published HCC database (24, 25). In contrast to their findings, by analyzing SIRT6 expression in 101 paired frozen HCC tissues and 60 paired paraffin-embedded sections, we convincingly showed that both SIRT6 mRNA and protein levels were significantly upregulated in the majority of HCC tissues compared with adjacent nontumoral liver tissues. Interestingly, high SIRT6 expression was associated with increased tumor grade, tumor size and vascular invasion. HCC patients with high SIRT6 expression showed significant correlation with poor overall survival rate. These clinical data suggests SIRT6 may act as an oncogene in HCC development. Unfortunately, the Marquardt study did not determine the expression of the SIRT6 in HCC clinical samples, which precluded a direct comparison between the two studies. We speculate that the different findings in these two studies may be due to different HCC population in different region. We also found that SIRT6 expression was low in three normal liver tissues and in PHH cells. SIRT6 suppression inhibited the growth

of HCC cells *in vitro* and *in vivo*. These data further support the pro-tumorigenic function of SIRT6 in HCC development.

The dysregulation or blockade of apoptosis machinery in cancer cells represents a potential mechanism of HCC carcinogenesis (26). Defects in the apoptosis pathway in cancer cells contribute to resistance to anticancer therapies (27). In terms of function, we found that SIRT6 suppression induced apoptosis in HCC cells and increased cell sensitivity to doxorubicin treatment. Concordantly, SIRT6 knockdown in human prostate cancer cells led to increased apoptosis and enhanced chemotherapeutic sensitivity(12). However, according to Meter et al., SIRT6 overexpression induces massive apoptosis in cancer cells, including fibrosarcoma, cervical carcinoma, primary breast tumor and metastatic breast tumor cell lines (28). This cell death requires the mono-ADP-ribosyltransferase but not the deacetylase activity of SIRT6 and is mediated by the activation of both the p53 and p73 apoptotic signaling cascades in cancer cells (28). Unfortunately, the study by Meter et al. did not include any liver cancer cell lines. Therefore, the function of SIRT6 in cancer may depend on tissue-specific molecular profiles.

We further revealed that SIRT6 contribute to the apoptosis process in hepatoma cells partially via Bax regulation. SIRT6 silencing also induced the expression of Smac, cytochrome C and cleaved Caspase-9, which are downstream effectors of Bax activation, suggesting that the Bax signaling pathway is active in SIRT6-depleted cells. Next, we observed that SIRT6 negatively regulates Bax transcription *via* H3K9 deacetylation. Our finding suggests a novel mechanism for SIRT6 in the epigenetic regulation of Bax *in* HCC cells. To our knowledge, this finding constitutes the first demonstration of a role for SIRT6 in gene expression *via* the modulation of chromatin in HCC. In the context of gene expression, acetylated H3K9 is associated with actively transcribed genes. In SIRT6-depleted cells, the hyperacetylation of H3K9 at the Bax promoter indeed enhanced the accessibility of transcription factors such as p53 to chromatin. Transcription factor p53 is a direct transcriptional activator of *Bax* gene (29, 30). In HCC cells, SIRT6 is recruited to promoter of *Bax* gene, deacetylates histone H3K9, decreases the accessibility of transcription factors such as p53 to

chromatin and thereby contributes to the termination of *Bax* transcription. However, whether SIRT6 physically interacted with transcription factors p53 needs our further investigation.

In summary, we demonstrated that SIRT6 acts as an oncogene in HCC development by blocking Bax expression and mitochondrial translocation. SIRT6 suppression also increased the sensitivity of liver cancer cells to chemotherapeutics. Our findings highlight the importance of the SIRT family in HCC carcinogenesis and provide useful tools for the development of mechanism-based cancer prevention strategies.

Acknowledgments

This study was supported by the National Natural Science Foundation of China (81472271 and 81270559), the National Science and Technology Major Project (2013ZX10002002), the Chongqing Natural Science Foundation (cstc2012jjA10047) and the Major project of Chongqing Science & Technology Commission (cstc2013jcyjC10002, ALH)

References

1. Shiraha H, Yamamoto K, Namba M. Human hepatocyte carcinogenesis (review). International journal of oncology. 2013;42:1133-8.

2. Schattenberg JM, Schuchmann M, Galle PR. Cell death and hepatocarcinogenesis: Dysregulation of apoptosis signaling pathways. Journal of gastroenterology and hepatology. 2011;26 Suppl 1:213-9.

3. Kelly GL, Strasser A. The essential role of evasion from cell death in cancer. Advances in cancer research. 2011;111:39-96.

4. Haigis MC, Guarente LP. Mammalian sirtuins--emerging roles in physiology, aging, and calorie restriction. Genes & development. 2006;20:2913-21.

5. Toiber D, Erdel F, Bouazoune K, Silberman DM, Zhong L, Mulligan P, et al. SIRT6 recruits SNF2H to DNA break sites, preventing genomic instability through chromatin remodeling. Molecular cell. 2013;51:454-68.

6. Kaidi A, Weinert BT, Choudhary C, Jackson SP. Human SIRT6 promotes DNA end resection through CtIP deacetylation. Science. 2010;329:1348-53.

7. Mao Z, Hine C, Tian X, Van Meter M, Au M, Vaidya A, et al. SIRT6 promotes DNA repair under stress by activating PARP1. Science. 2011;332:1443-6.

8. Michishita E, McCord RA, Berber E, Kioi M, Padilla-Nash H, Damian M, et al. SIRT6 is a histone H3 lysine 9 deacetylase that modulates telomeric chromatin. Nature. 2008;452:492-6.

9. Kawahara TL, Michishita E, Adler AS, Damian M, Berber E, Lin M, et al. SIRT6 links histone H3 lysine 9 deacetylation to NF-kappaB-dependent gene expression and organismal life span. Cell. 2009;136:62-74.

10. Khongkow M, Olmos Y, Gong C, Gomes AR, Monteiro LJ, Yague E, et al. SIRT6 modulates paclitaxel and epirubicin resistance and survival in breast cancer. Carcinogenesis. 2013;34:1476-86.

11. Ming M, Han W, Zhao B, Sundaresan NR, Deng CX, Gupta MP, et al. SIRT6 Promotes COX-2 Expression and Acts as an Oncogene in Skin Cancer. Cancer research. 2014;74:5925-33.

12. Liu Y, Xie QR, Wang B, Shao J, Zhang T, Liu T, et al. Inhibition of SIRT6 in prostate cancer reduces cell viability and increases sensitivity to chemotherapeutics. Protein & cell. 2013.

13. Han Z, Liu L, Liu Y, Li S. Sirtuin SIRT6 suppresses cell proliferation through inhibition of Twist1 expression in non-small cell lung cancer. International journal of clinical and experimental pathology. 2014;7:4774-81.

14. Bauer I, Grozio A, Lasiglie D, Basile G, Sturla L, Magnone M, et al. The NAD+-dependent histone deacetylase SIRT6 promotes cytokine production and migration in pancreatic cancer cells by regulating Ca2+ responses. The Journal of biological chemistry. 2012;287:40924-37.

15. Chen X, Hao B, Liu Y, Dai D, Han G, Li Y, et al. The histone deacetylase SIRT6 suppresses the expression of the RNA-binding protein PCBP2 in glioma. Biochemical and biophysical research communications. 2014;446:364-9.

16. Min L, Ji Y, Bakiri L, Qiu Z, Cen J, Chen X, et al. Liver cancer initiation is controlled by AP-1 through SIRT6-dependent inhibition of survivin. Nature cell biology. 2012;14:1203-11.

17. Lefort K, Brooks Y, Ostano P, Cario-Andre M, Calpini V, Guinea-Viniegra J, et al. A miR-34a-SIRT6 axis in the squamous cell differentiation network. The EMBO journal. 2013;32:2248-63.

18. Sebastian C, Zwaans BM, Silberman DM, Gymrek M, Goren A, Zhong L, et al. The histone deacetylase SIRT6 is a tumor suppressor that controls cancer metabolism. Cell. 2012;151:1185-99.

19. Chen J, Zhang B, Wong N, Lo AW, To KF, Chan AW, et al. Sirtuin 1 is upregulated in a subset of hepatocellular carcinomas where it is essential for telomere maintenance and tumor cell growth.

Cancer research. 2011;71:4138-49.

20. Chen J, Chan AW, To KF, Chen W, Zhang Z, Ren J, et al. SIRT2 overexpression in hepatocellular carcinoma mediates epithelial to mesenchymal transition by protein kinase B/glycogen synthase kinase-3beta/beta-catenin signaling. Hepatology. 2013;57:2287-98.

21. Law BY, Wang M, Ma DL, Al-Mousa F, Michelangeli F, Cheng SH, et al. Alisol B, a novel inhibitor of the sarcoplasmic/endoplasmic reticulum Ca(2+) ATPase pump, induces autophagy, endoplasmic reticulum stress, and apoptosis. Molecular cancer therapeutics. 2010;9:718-30.

22. Lavorato-Rocha AM, Anjos LG, Cunha IW, Vassallo J, Soares FA, Rocha RM. Immunohistochemical assessment of PTEN in vulvar cancer: best practices for tissue staining, evaluation, and clinical association. Methods. 2015;77-78:20-4.

23. Lai CC, Lin PM, Lin SF, Hsu CH, Lin HC, Hu ML, et al. Altered expression of SIRT gene family in head and neck squamous cell carcinoma. Tumour biology : the journal of the International Society for Oncodevelopmental Biology and Medicine. 2013;34:1847-54.

24. Marquardt JU, Fischer K, Baus K, Kashyap A, Ma S, Krupp M, et al. Sirtuin-6-dependent genetic and epigenetic alterations are associated with poor clinical outcome in hepatocellular carcinoma patients. Hepatology. 2013;58:1054-64.

25. Andersen JB, Factor VM, Marquardt JU, Raggi C, Lee YH, Seo D, et al. An integrated genomic and epigenomic approach predicts therapeutic response to zebularine in human liver cancer. Science translational medicine. 2010;2:54ra77.

26. Fabregat I, Roncero C, Fernandez M. Survival and apoptosis: a dysregulated balance in liver cancer. Liver international : official journal of the International Association for the Study of the Liver. 2007;27:155-62.

27. Tsuruo T, Naito M, Tomida A, Fujita N, Mashima T, Sakamoto H, et al. Molecular targeting therapy of cancer: drug resistance, apoptosis and survival signal. Cancer science. 2003;94:15-21.

28. Van Meter M, Mao Z, Gorbunova V, Seluanov A. SIRT6 overexpression induces massive apoptosis in cancer cells but not in normal cells. Cell Cycle. 2011;10:3153-8.

29. Moll UM, Wolff S, Speidel D, Deppert W. Transcription-independent pro-apoptotic functions of p53. Current opinion in cell biology. 2005;17:631-6.

30. Speidel D. Transcription-independent p53 apoptosis: an alternative route to death. Trends in cell biology. 2010;20:14-24.

Figure legends

Fig.1 Differential expression of SIRT6 in HCC samples. (A-B) SIRT6 mRNA and protein expression in 6 liver cancer cell lines, the immortalized liver cell line (MIHA) and primary human hepatocyte (PHH). β-actin (43kDa) was used as a reference gene for real-time PCR and as a loading control for western blot analysis. (C) Immunohistochemical examination of SIRT6 in 60 paired primary HCC tissues and adjacent nontumoral tissues. Magnification, ×400. (D) Western blot analysis of SIRT6 (37kDa) in 101 paired frozen HCC tissues (T) and adjacent non-tumor liver tissues (N). β-actin was used as a loading control. (E) Quantitative analysis of SIRT6 protein levels in 101 paired HCC tissues. *, $p<0.01$. (F) Real-time PCR analysis of SIRT6 mRNA levels in 101 paired HCC tissues and adjacent nontumoral tissues. β-actin mRNA expression was used as an internal control. *, $p<0.01$. (G) Kaplan-Meier analysis of overall survival in 53 HCC patients based on SIRT6 expression.

Fig.2 SIRT6 depletion inhibits HCC cell growth and induces apoptosis. (A) SIRT6 protein expression in HCC cells was significantly inhibited by lentivirus expressing SIRT6-targeting shRNA (shSIRT6-1 and shSIRT6-2) versus control (shCont) shRNA. Cells were harvested 3 days after virus infection. β-actin was used as a loading control. (B) SIRT6 knockdown significantly inhibited the proliferation of HCC cells. PLC/PRF/5, SK-Hep-1, SMMC-7721 and Huh-7 cells were infected with lentivirus, and cell numbers were determined by a trypan blue exclusion assay at the indicated number of days thereafter. Plots represent cumulative cell numbers versus days in culture. *, $p<0.001$. (C) SIRT6 knockdown reduced colony formation. SK-Hep-1 cells infected with lentivirus as indicated were cultured for 2 weeks in the presence of blasticidin (3.5μg/mL) and stained with crystal violet. Quantification of colonies were obtained from macroscopically visible colonies in each well and expressed as percentage relative to the control group. *, $p<0.001$. (D) An EdU incorporation assay was used to analyze cell proliferation. The quantification of EdU-positive cells was conducted macroscopically and expressed as a percentage relative to the control cells. *, $p<0.01$. (E) SIRT6 silencing induced apoptosis in SK-Hep-1 and Huh-7 cells. Apoptosis in different groups was analyzed by flow

cytometry with Annexin V/PI (E). *, $p<0.01$. All histograms show mean values from 3 independent experiments; bars indicate SD. (F) Apoptosis in different groups was analyzed by PARP cleavage and Caspase-3 cleavage analysis. PARP: 116 kDa; Cleaved PARP: 89 kDa; Caspase-3: 35 kDa; Cleaved Caspase-3: 19 kDa.

Fig.3 SIRT6 regulates cell apoptosis *via* Bax signaling. (A) SIRT6 regulated Bax mRNA (Left panel) and protein levels (Right panel) in SK-Hep-1, Huh-7 cells and MIHA cells. *, $p<0.01$. (B) Western blot analysis of several components of the Bax-mediated apoptotic pathway in SIRT6-depleted cells. β-actin was used as a loading control. Bax: 20 kDa; Bcl-2: 26 kDa; Smac: 21 kDa; Cytochrome c: 14 kDa; Caspase-9: 49 kDa; Cleaved Caspase-3: 37,39 kDa. (C) Immunofluorescence analysis of Bax (green) and mitochondria (red) in SIRT6-depleted SK-Hep-1 cells showed that SIRT6 promoted the mitochondrial translocation of Bax. (D)Western blotting analysis of Bax in cytosolic, mitochondrial and nuclear fractions of SK-Hep-1 cells expressing shSIRT6 or shCont. COX IV(17kDa), GAPDH (37kDa) and Histone H3(17kDa) were used as markers for the mitochondrial, cytosolic and nuclear fractions, respectively. (E) Gene silencing of Bax rescued the growth inhibition induced by SIRT6 depletion in SK-Hep-1 cells. Cell numbers were counted 4 days after transfection using a trypan blue exclusion assay. *, $p<0.01$. (F-G) Bax suppression abolished the induction of apoptosis in SIRT6-depleted SK-Hep-1 cells. Apoptosis in different groups was analyzed by flow cytometry with Annexin V/PI (F) and by PARP cleavage analysis (G). *, $p<0.01$. All histograms show mean values from 3 independent experiments; bars indicate SD.

Fig. 4 SIRT6 regulates Bax gene expression *via* the deacetylation of H3 Lysine 9. (A) The promoter activity of the Bax gene was measured using a dual-luciferase reporter assay. SK-Hep-1, Huh-7 and MIHA cells were transfected with pGL3-basic or reporter constructs containing various lengths of the 5'-flanking region of the Bax gene as indicated. The data are presented as the mean±SD of three independent experiments. (B) SIRT6 depletion activated the Bax promoter. SK-Hep-1 and Huh-7cells were transfected with pGL3-982, pGL3-803, pGL3-588, pGL3-389 and pGL3-213 after infection with lentivirus expressing shSIRT6. The data are presented

as the mean±SD of three independent experiments. *, $p<0.01$. (C) ChIP assay was performed to confirm the interaction between SIRT6 and the promoter region of Bax. (D) SIRT6 is required for H3K9 deacetylation at the Bax promoter. ChIP assay with anti-H3K9Ac or anti-H4K16Ac was performed in SK-Hep-1 cells infected with lentivirus expressing shSIRT6 or shCont; H3K9 or H4K16 acetylation at the Bax promoter (mean±SD) is shown relative to input. $p<0.01$. (E) SIRT6 silencing promoted transcription factor p53 and E2F-1 occupancy at the promoter of Bax gene. ChIP assay with anti-p53 or E2F-1 was performed in SK-Hep-1 cells. p53 or E2F-1 occupancy (mean±SD) at promoter in SIRT6-depleted cells relative to input is shown.*, $p<0.01$. All histograms show mean values from 3 independent experiments; bars indicate SD.

Fig.5 SIRT6 depletion inhibited HCC growth *in vivo*. SK-Hep-1 cells infected with lentivirus expressing shSIRT6, shSIRT6+shBax or shCont were injected subcutaneously into 4-week-old nude mice. At 4 weeks after implantation, the animals were sacrificed, and the tumor masses were excised. (A) Analysis of tumor volume over a 4-week time course. The data represent the mean±SD. *, $p<0.001$. (B) Representative images of tumors formed by the implantation of SK-Hep-1 cells expressing shSIRT6, shSIRT6+shBax or shCont. (C) Tumor weights in different groups of nude mice. Data represent the mean±SD. Bars indicate SD;*, $p<0.001$. (D) Representative images of immunohistochemical staining of SIRT6, Bax, cleaved PARP and Ki67 in tumor xenografts with hematoxylin counterstaining. Magnification, ×400. Quantification of positive cells was calculated based on HScore formula. *, $p<0.01$. (E) Correlation analysis SIRT6 mRNA and Bax mRNA in 101frozen HCC tissues. SIRT6 and Bax mRNA was first normalized by the expression level of β-actin, and the induction of SIRT6 and Bax in HCC over nontumoral liver in each patients was calculated. Correlation analysis was analyzed by Spearman's σ rank test.

Table 1.Correlative analysis of SIRT6 protein levels with clinico-pathological features. High tumoral SIRT6 expression was considered >1.5-fold up-regulation relative to the adjacent non-tumoral liver.

Table1.Correlation of SIRT6 expression with clinicopathologic features

Clinicopatholigic Parameters	No.of Specimens	SIRT6 Expression (Tumor/Nontumoral) Low	High	*P* Value
Sex				
Female	14	2	12	0.13
Male	87	32	55	
Age(mean±SD)		52.5±13.6	53.9±11.6	0.59
ALT				
≤40 IU/L	46	14	32	0.53
＞40IU/L	55	20	35	
CEA				
≤5ng/mL	80	27	53	0.97
>5ng/mL	21	7	14	
AFP				
≤20 ng/mL	55	15	40	0.14
＞20 ng/mL	46	19	27	
Tumor size				
≤3 cm	25	13	12	0.02
＞3 cm	76	21	55	
Multiple Tumor				
No	71	25	46	0.61
Yes	30	9	21	
Grade				
1	13	8	5	0.02
2	69	23	46	
3	19	3	16	
Vascular invasion				
No	71	30	41	0.004
Yes	30	4	26	
Cirrhosis				
No	52	25	27	0.34
Yes	49	19	30	

Author Manuscript Published OnlineFirst on February 9, 2016; DOI: 10.1158/1078-0432.CCR-15-1638
Author manuscripts have been peer reviewed and accepted for publication but have not yet been edited.

Figure 1

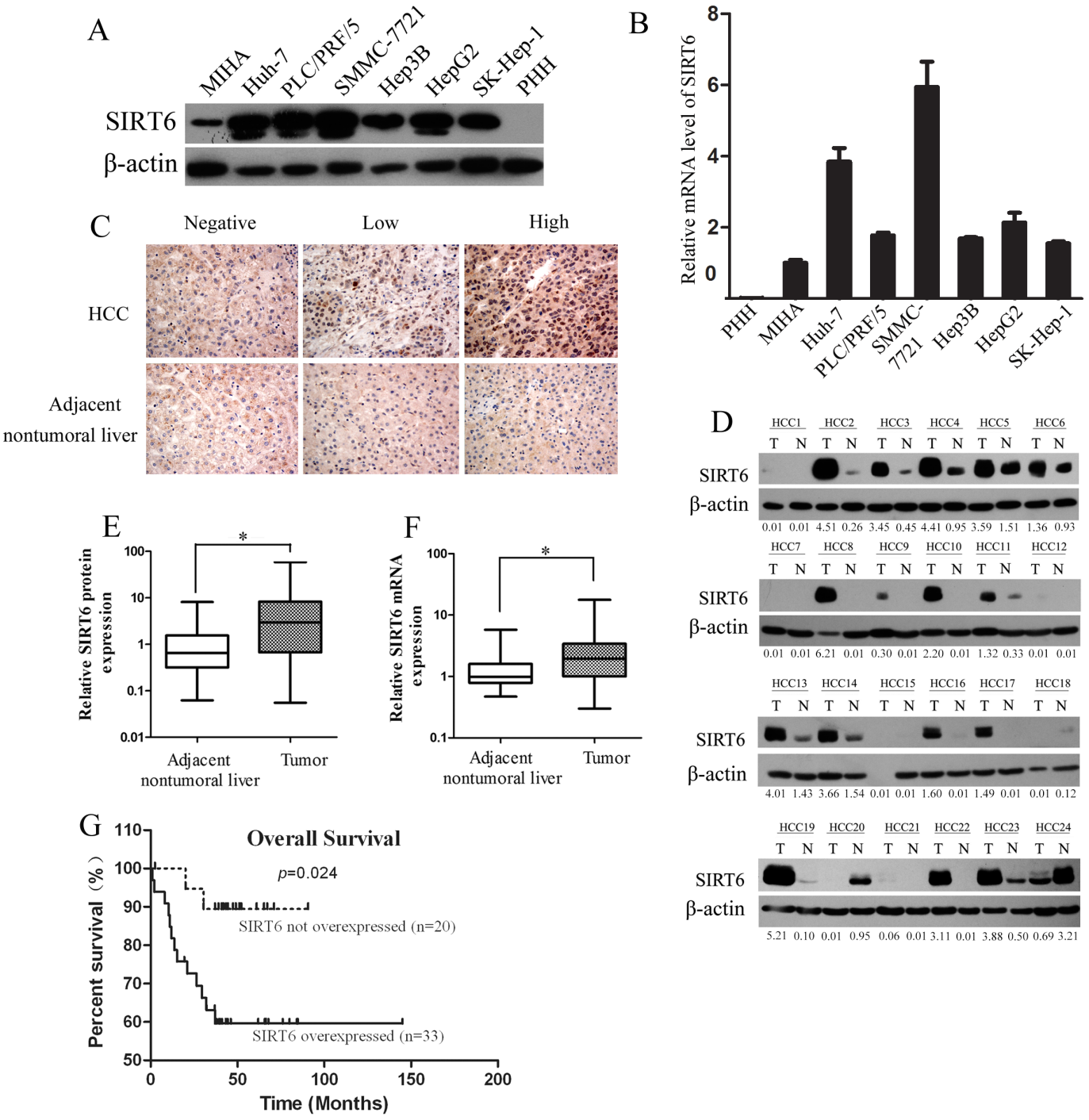

Figure 2

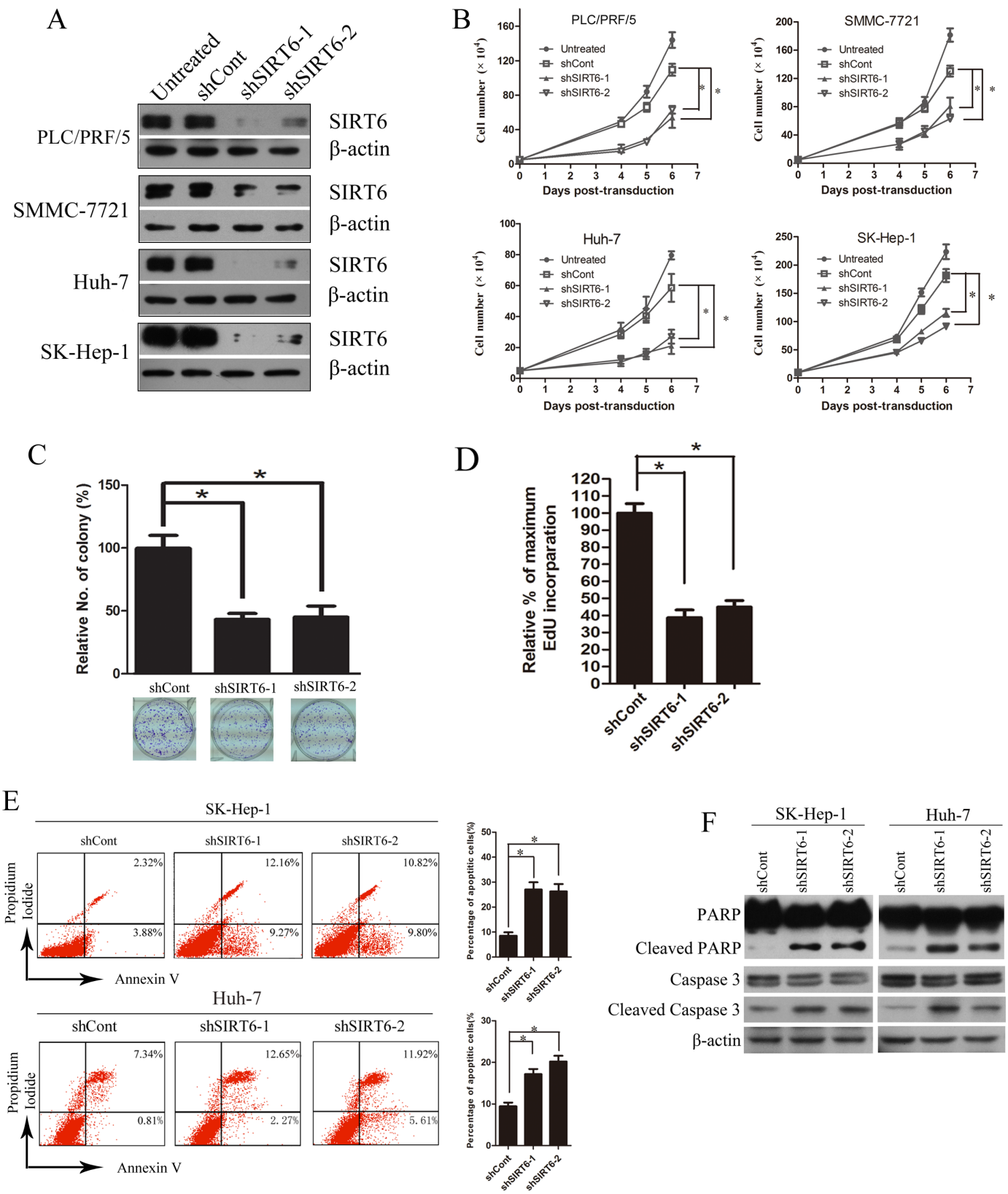

Author Manuscript Published OnlineFirst on February 9, 2016; DOI: 10.1158/1078-0432.CCR-15-1638
Author manuscripts have been peer reviewed and accepted for publication but have not yet been edited.

Figure 3

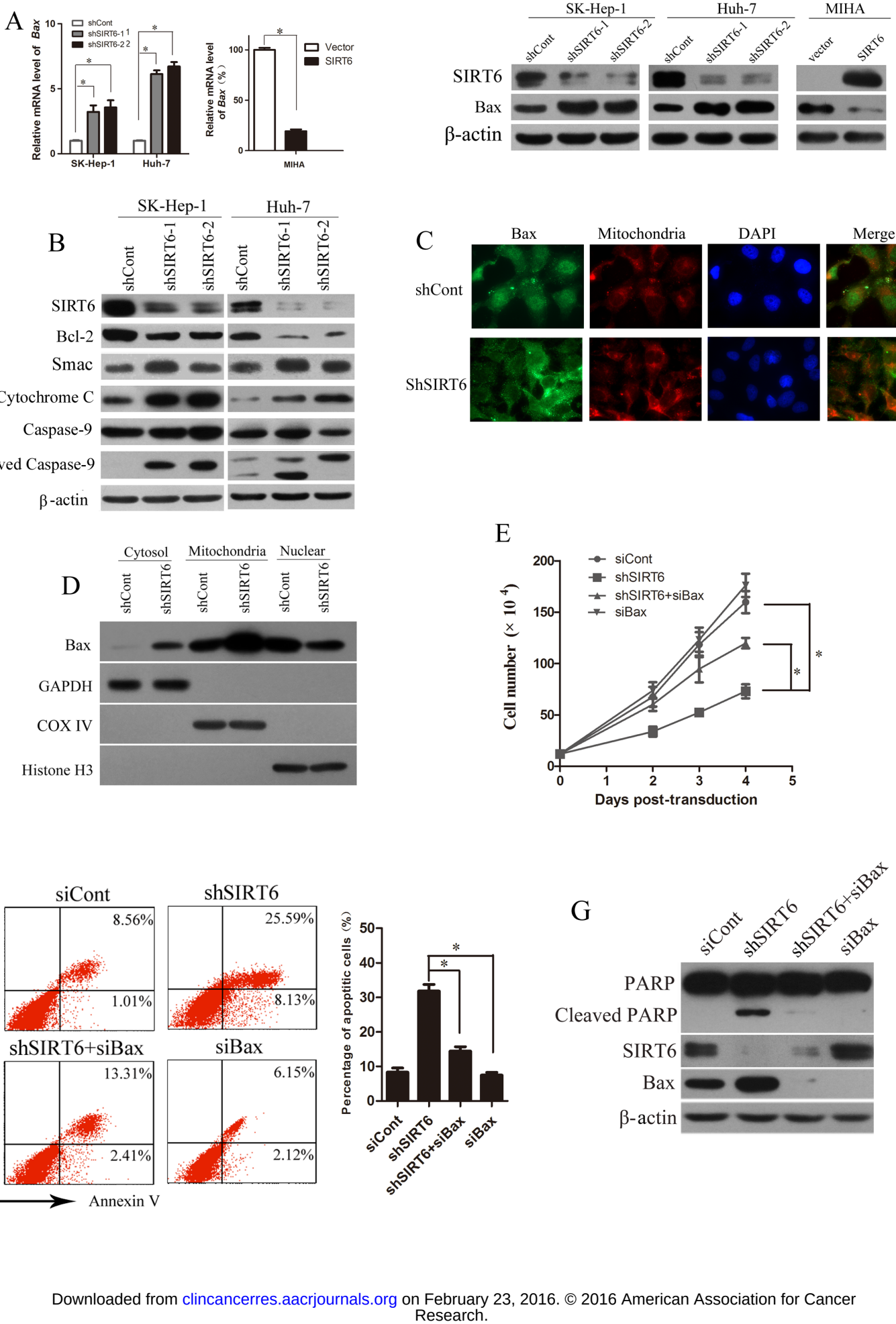

Author Manuscript Published OnlineFirst on February 9, 2016; DOI: 10.1158/1078-0432.CCR-15-1638
Author manuscripts have been peer reviewed and accepted for publication but have not yet been edited.

Figure 4

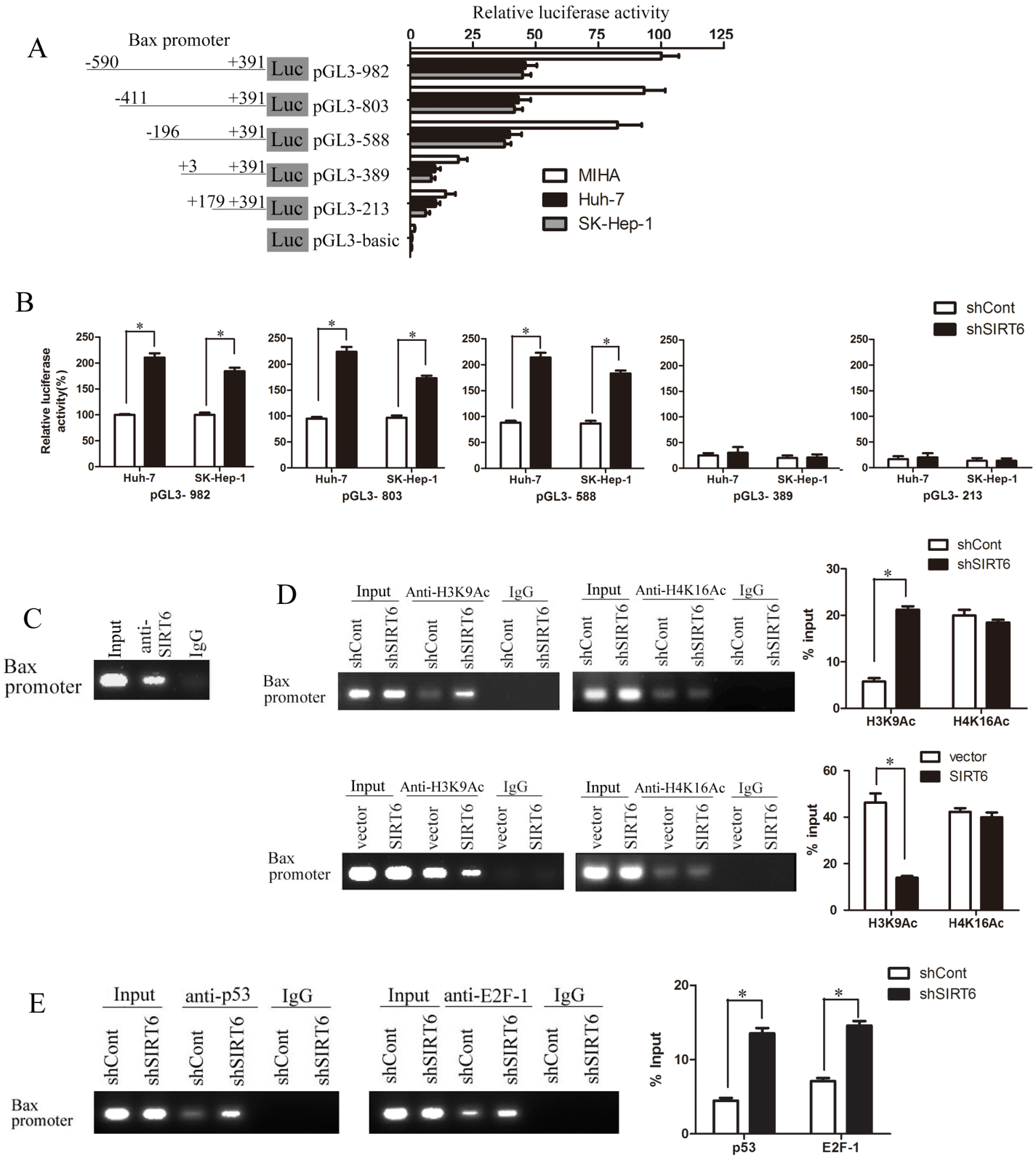

Author Manuscript Published OnlineFirst on February 9, 2016; DOI: 10.1158/1078-0432.CCR-15-1638
Author manuscripts have been peer reviewed and accepted for publication but have not yet been edited.

Figure 5

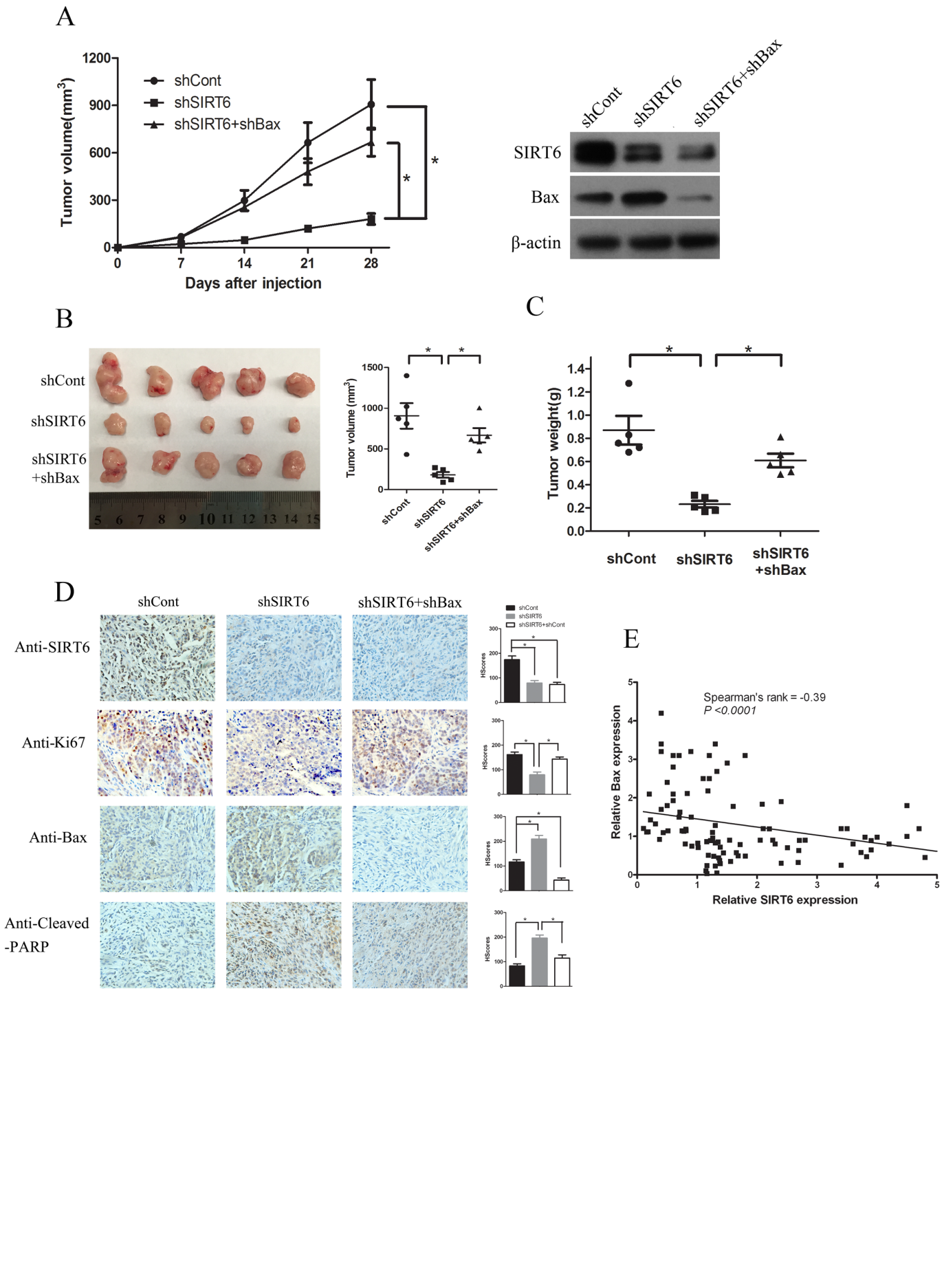

AACR American Association for Cancer Research

Clinical Cancer Research

SIRT6 overexpression potentiates apoptosis evasion in hepatocellular carcinoma via BCL2-associated X protein-dependent apoptotic pathway

Juan Chen, Rong-Kuan Ran, Yong Chen, et al.

Clin Cancer Res Published OnlineFirst February 9, 2016.